

THE 4TH INTERNATIONAL CONFERENCE ON ALUMINUM ALLOYS

INFLUENCE OF THE ASPECT RATIO DISTRIBUTION ON THE DAMAGE MECHANISMS IN AN OSPREY™ Al ALLOY - SiC_p COMPOSITE.

E. Maire, C. Verdu, G. Lormand and R. Fougères.
GEMPPM, URA CNRS n°341, INSA-Lyon Bât. 303. 20, avenue Albert Einstein F-69621
Villeurbanne Cedex - France.

Abstract

In situ tensile tests have been performed on a 7049 Al alloy + 15 % SiC particulate reinforced metal matrix composite in order to study the damage mechanisms in this kind of material. Gold microgrids have been deposited on the polished surface of the specimen as an indicator of the modifications induced by the damaging phenomena. The most elongated particles tend to be cracked easily. An Eshelby iterative model has been used to calculate the stress field induced in the inclusions by the thermomechanical treatment and mechanical loading. This method has permitted to take the interactions between particles with different aspect ratio into account in the calculation of the stress field. The comparison between the normal stress in the most and the less elongated particles led to a good explanation of the experimental results.

Introduction

Metal Matrix Composites have been widely studied because their elastic properties (Young modulus and yield stress) are higher than these of the unreinforced metal used for the matrix. Among all the systems investigated up to now, particulate reinforced MMCs appear to be the more interesting because of the low price and quite good formability of the products. The counterpart of the high elastic properties of these materials is the loss of ductility and fracture toughness. Several authors [1-6] have used in situ tensile tests to study the rupture of micro heterogeneous materials. These mechanical tests (tensile tests most of the time) are performed in situ in the microscopes (optical or Scanning Electron microscopes). They permit to analyse the deformation mechanisms, from the first stages of the damage up to the final fracture of the sample. The aim of this study is to describe failure mechanisms of a particulate MMC obtained by the OSPREY™ route by using SEM in situ tensile tests and then to analyse the experimental results by means of a model based on the Eshelby method [7], which is well adapted to the calculation of the elastic stress fields in this kind of materials.

Material - Microstructure

The studied material is a 7049 aluminium alloy reinforced with 15% vol. SiC particles. It is obtained by the OSPREY™ route [8]. The thermal treatment corresponds to the classical

overaging treatment of the unreinforced matrix : 475°C 1h, cold water quench, 24 h. 120°C and 8 h. 160°C. As one can note on the figure 1, the particles are located at random in the matrix. Their aspect ratio is largely scattered around a mean value which is close to 2. After extrusion the particles are aligned according to the extrusion axis. This axis is also the tension axis during the tensile loading. The microstructure of the composite matrix has been also investigated by SEM and TEM observations. The grain size of these OSPREY™ composites, is very small (3 μm). A classical precipitate free zone (PFZ) of 40 nm width has been observed at the grain boundaries and at the particle/matrix interface.

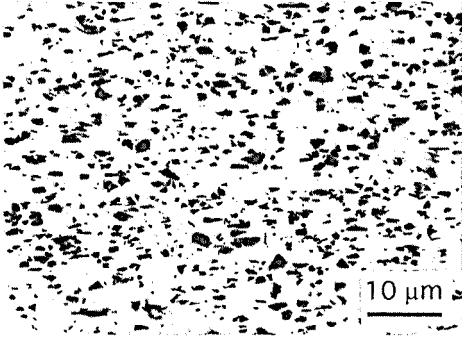


Figure 1: Optical micrograph of the studied composite showing the particle aspect ratio distribution.

Tensile conditions. Samples

The shape of the tensile specimen (figure 2), has been designed to minimise the stress concentration in the region of the sample where the SEM observations are performed.

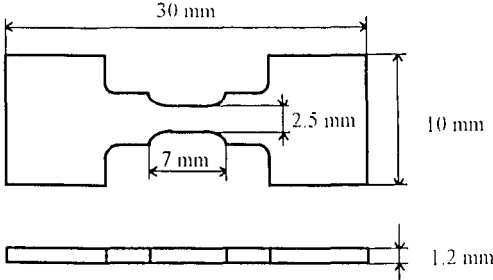


Figure 2: Shape of the samples used for the SEM in situ tensile tests

Square gold microgrids are deposited on the polished and etched surface of the specimens. They are helpful for the analysis of the plastic deformation modes of the matrix, and for the measurement of the local plastic deformations (an example of microgrids can be seen in figure 3). Further details concerning the grid elaboration can be found in reference [4]. The tests have been performed in a JEOL 840A type SEM with a tensile loading device fixed on the SEM goniometric

stage. This sensitive device allows the observation zone to be kept fixed during the loading, the motion of the two grips being symmetrical.

Results

Figure 3 and 4 are SEM micrographs of a same zone before and during the loading.

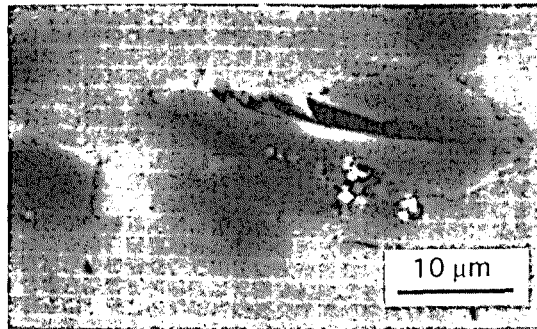


Figure 3: Initial state of the observed zone. The {3} axis (tensile axis) is horizontal. $\sigma = 0$ Mpa, $\epsilon_p = 0$ %. Note the presence of gold microgrids as a network of white lines.



Figure 4: Particle cracking (same zone). $\sigma = 600$ Mpa, $\epsilon_p = 0.01$ %. Note the deformation of microgrids near the particle crack.

Damage initiation

The main damage initiation mechanism corresponds to the fracture of the SiC particles (figure 4). Particle debondings are also observed, but they occur less frequently, and generally at more important values of the plastic strain. The first particle cracks are observed in the composite material for an average plastic strain of the sample $\epsilon_p = 0.01$ % and an applied stress $\sigma_a = 600$ Mpa (below the yield stress of the composite which is $\sigma_{0.2} = 635$ Mpa). The cracks in the SiC particles occurs most of the time perpendicularly to the tension axis. We have observed that the big and elongated particles were more prone to crack than the small and spherical ones. This has also been reported by Llorca [9] and by Zhong [10].

Damage growth and fracture

As the applied stress is increased, the number of cracked particles increases. The width of the initial cracks also increases. The aspect of these cracks becomes rectangular. This can occur because the stress field in front of the crack tip is important. Therefore dislocations are emitted in directions roughly equal to 45° to the crack plane, leading to very strong local shear deformation bands in the matrix (see figure 4). Using the deformation of the gold grids, we have measured a plastic shear strain of $\approx 12\%$ in the bands (the average tensile deformation of the sample at this point was 3% only).

Rupture of the sample

Post rupture observations of etched samples near the fracture permit to show that in our case, the junction between the first cracks is intergranular: the crack in the matrix which links the first damages and then leads to the final rupture is observed to be located near the grain boundaries (see figure 5).

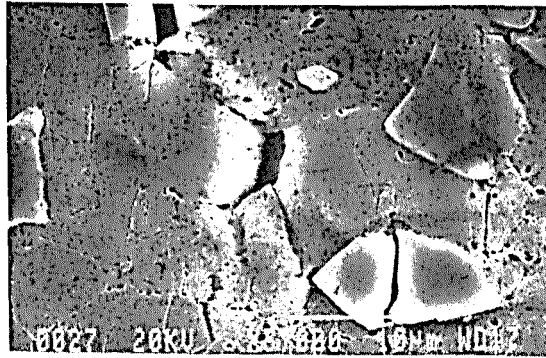


Figure 5: Post rupture observation of the fracture zone showing the intergranular propagation of the final crack.

Discussion

Damage initiation

A particle breaks when the stress field in it reaches a critical level so the value of this stress field appears to have a great importance on the damage initiation. This stress field is due to deformation incompatibilities between particles and matrix made of materials having different intrinsic properties. **Thermal** incompatibilities arise during the cooling of the sample due to the mismatch of the coefficients of thermal expansion. **Elastic** incompatibilities increase during the loading due to the mismatch of the Young modulus. **Plastic** incompatibilities are due to the fact that the matrix exhibits plastic deformation while the particles remain elastic. In order to explain in a theoretical way, some of the observed experimental phenomena arising in the damage initiation domain, we have used an Eshelby iterative model (described in reference [11]) which permits to calculate this internal stress field. In this model, particle reinforcements are divided into several families. Each particle of the family is supposed to have the same Young modulus, aspect ratio and disorientation to the applied tensile axis than the others. In our experimental observations, the particle crack planes are observed to be perpendicular to the tensile axis. Thus, it has been chosen to focus the analysis on the value of the **normal** stress (rather than the Tresca

or the Von Mises stress). Firstly, we consider that the incompatibilities mentioned above are relaxed by **elastic** stresses. Plastic relaxation will also be discussed but in a qualitative way. After the solution heat treatment (475°C 1h.) and just before the quench it can be assumed that the material is in a reference state: the internal stresses in the body of the sample are completely relaxed. The thermomechanical properties of the two constituents used for the calculations are $E=72$ Gpa, $\nu=0.2$ and $\alpha=23.5 \cdot 10^{-6}/^\circ$ for the 7049 alloy and $E=402$ Gpa $\pm 2\%$ (*), $\nu=0.2$ and $\alpha=3.5 \cdot 10^{-6}/^\circ$ for the SiC. The value of Young modulus of the SiC particle is quite difficult to choose because there is a large scatter in the properties reported in the literature. The value chosen here (*) has been determined experimentally in our laboratory by means of in situ nanoindentation experiments [12]. We firstly quantify the normal stress that can be induced by the three different incompatibilities separately. We do this first for a ideal composite reinforced with a single family of SiC particles supposed to have an aspect ratio of 2 and a volume fraction of 15%. Figures 6, 7 and 8 show the evolution of the normal stress component in the SiC particles versus the temperature gap, the stress applied and the plastic strain of the sample respectively. The arrows on the three curves indicate the corresponding values for our experimental observations (concerning the first damages).

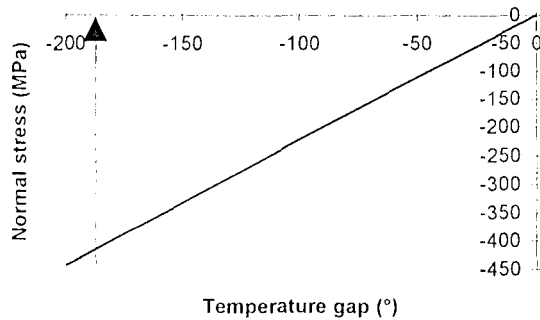


Figure 6: Normal stress versus the temperature gap (1 family : Vf = 15 %, s = 2).

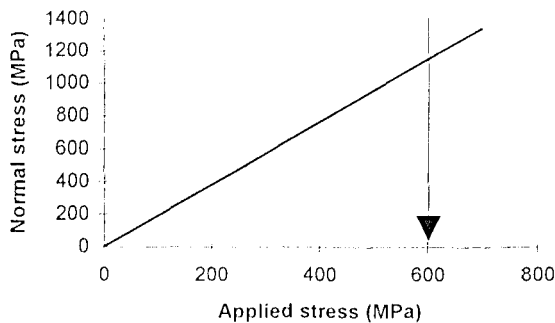


Figure 7: Normal stress versus the applied stress (1 family : Vf = 15 %, s = 2).

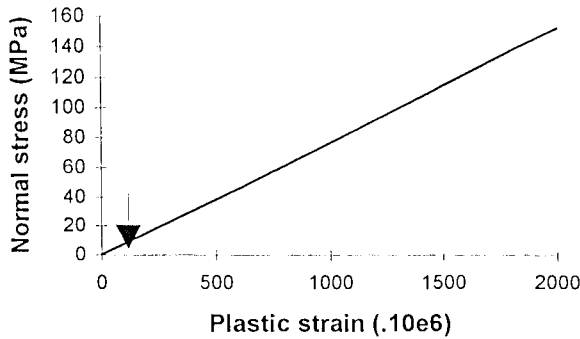


Figure 8: Normal stress versus the plastic strain of the sample (1 family : $V_f = 15\%$, $s = 2$).

The thermal cooling induces a compressive normal stress component. This compressive stress can delay the rupture of the considered particle. On the other hand the applied stress and the plastic deformation of the sample induce tensile normal stresses in the particles, that accelerate the rupture. Note that the plastic incompatibility can become very high, but as far as the first damages are considered, it is neglectable.

The stress field in a given particle depends also on other factors such as its aspect ratio and the location of the surrounding particles. Thus, the use of several families for the realistic description of the composite is interesting. From surface observations of a large amount of particles, the distribution of the particle aspect ratio has been experimentally determined (see table I). This distribution can be modelled by 15 classes (families) of particles. Each class has a mean aspect ratio and a volume fraction in the composite.

The figure 9 shows the evolution of the normal stress versus the stress applied for three particular families of inclusions ($s=1.25$, 2.25 and 7.25). The stress field in **each** family depends of course on the volume fraction and aspect ratio of the **other** families.

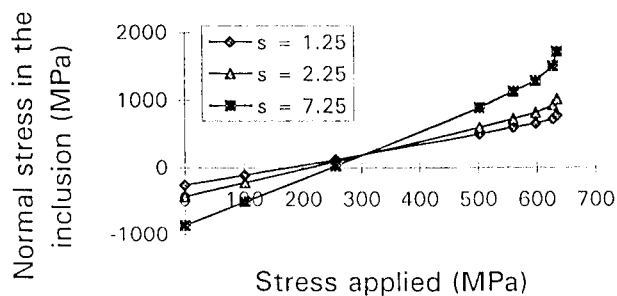


Figure 9 : Normal stresses versus the applied stress in three different families of SiC inclusions ($s=1.25$, $s=2.25$ and $s=7.25$). The elastic, plastic and thermal incompatibilities are relaxed by elastic stresses.

s	0.25	0.75	1.25	1.75	2.25	2.75	3.25	3.75	4.25	4.75	5.25	5.72	6.25	6.75	7.25
Vf (%)	0.02	1.25	3.59	2.42	2.65	1.79	1.17	0.70	0.62	0.23	0.15	0	0.08	0	0.08

Table 1: aspect ratio distribution of the SiC particles, experimentally determined by means of surface observations. This distribution is divided into 15 classes, each one having a mean aspect ratio and a volume fraction in the composite. The stress field in the **3 particular classes** is studied in figure 9.

Before the tensile loading of the composite ($\sigma_a=0$), the SiC particles exhibit a normal compression stress component, due to the thermal incompatibility induced by the cooling. As it can be seen in the figure 9, the longest particles (high aspect ratio) are the most compressed. Therefore at the beginning of the tensile loading, the risk of damage is reduced in these particles. However as the applied stress is increased, the normal stress σ_{33} in the elongated particles increases more rapidly than in the spherical particles. For an applied tensile stress σ_a of 300 MPa, all the particles are submitted to a tensile stress according to the tensile axis. The normal stress within the elongated particles becomes then higher than this within the other particles. As particle cracks have been observed at an applied stress of 600 MPa, it is clear from this theoretical consideration that the first broken particles are the most elongated ones. This is in good agreement with experimental observations.

Plastic relaxation

We have assumed in the calculations that the relaxation of the incompatibilities are completely elastic. In reality, the compressive stresses in the inclusions are probably reduced because the thermal incompatibilities in the matrix are relaxed by the emission of dislocations during the cooling that follows the ageing treatment. This occurs mainly in the case of the elongated particles, in which the internal stress field is very important. Thus the initial difference between the spherical and the elongated inclusions should be smaller. When the load is applied, the normal stresses grow with the same slopes than these of the curves in figure 9. This suggests that the tension normal stress corresponding to the damage initiation is more important for the elongated particles even if plastic relaxation occurs. Therefore, conclusions drawn from the elastic relaxation hypothesis are confirmed when plastic relaxation is considered.

Particle size influence

As it is often reported in the literature [2,10], we experimentally observed that the size of the particles have an important effect on their cracking probability. This problem is not solved in the literature yet. Unfortunately, the kind of model we use cannot describe this effect: as a matter of fact the value of the stress field calculated from the Eshelby method does not depend on the size of the particles. The size effect may be explained by the fact that the SiC particle cracking occurs probably from defects resulting from the fabrication of these particles and that the big particles are likely to contain more defects than the small ones.

Conclusion

SEM in situ tensile tests have been used to study the damage mechanisms in a 7049 aluminium alloy-SiCp composite. This mechanism can be divided into different steps:

- The damage initiation occurs mainly by elongated SiC particle cracking.

- The number of these damage sites increases if the applied stress increases. The aspect of the first initiated cracks becomes rectangular.
- The fracture of the sample occurs by joining together the damage sites, by nucleation and growth of cracks in the matrix.
- These junction cracks are intergranular.

The calculation of the stress field in the inclusions induced by the complex thermo mechanical loading of the composite has been achieved by means of an Eshelby iterative method, firstly for an ideal description of the composite (in order to quantify the contribution of each incompatibility) and then for a more realistic description. The interaction between the different families of inclusions has been taken into account and the measured value of the SiC has been used for the calculation. This has permitted us to explain why the elongated particles tend to crack easily.

Acknowledgements

This work was financially supported by the Commission of the European Communities and all the partners of the European Brite contract: "Low cost MMC made by Spray Deposition", which are fully acknowledged.

References

1. F. J. Humphreys. Proceedings of the congress: 'EMAG MICRO 89', London, (Sept. 1989), 465.
2. N. Kanetake and T. Choh. Proceedings of the congress: 'ICCM9', Madrid, (July 1993), 634.
3. A. Mocellin, R. Fougères, P. F. Gobin. Journal of Materials Science, **28**, (1993), 4855.
4. M. H. Ambroise, T. Bretheau and A. Zaoui. In 'Micromechanics and homogeneity', Edited by G. J. Weng, M. Taya and H. Abe (New York 1990), 41.
5. M. Manoharan, J. J. Lewandowski. Scripta metallurgica **23**, (1989), 1801.
6. C. S. Lee, Y. H. Kim, T. Lim, K. S. Han. Scripta Metall. Mater. **25**, (1991), 613.
7. J. D. Eshelby. Progress in solid mechanics (Edited by I. N. Sneddon and R. Hill). North-Holland, Amsterdam, (1961), 89.
8. A. R. E. Singer. Mat. Sc. Engng. **A135**, (1991), 13.
9. J. Llorca, A. Martin, J. Ruiz and M. Elices. Met. Trans. A. **24**, (1993), 1575.
10. Y. Zong and B. Derby. Proceedings of the congress 'Euromat 93', Paris, (June 93), 1861
11. R. Hamann, A. Mocellin, P.F. Gobin and R. Fougères. Scripta Metall. Mater. **26**, (1992), 963.
12. W. C. Oliver, G. M. Phar. J. Mat. Res. **7**, (1992), 1565